

Stretchable and Flexible Buckypaper-Based Lactate Biofuel Cell for Wearable Electronics

Xiaohong Chen, Lu Yin, Jian Lv, Andrew J. Gross, Minh Le, Nathaniel Georg Gutierrez, Yang Li, Itthipon Jeerapan, Fabien Giroud, Anastasiia Berezovska, Rachel K. O'Reilly, Sheng Xu, Serge Cosnier,* and Joseph Wang*

This work demonstrates a stretchable and flexible lactate/O₂ biofuel cell (BFC) using buckypaper (BP) composed of multi-walled carbon nanotubes as the electrode material. Free-standing BP, functionalized with a pyrene-polynorborene homopolymer, is fabricated as the immobilization matrix for lactate oxidase (LOx) at the anode and bilirubin oxidase at the cathode. This biofuel cell delivers an open circuit voltage of 0.74 V and a high-power density of 520 μW cm⁻². The functionalized BP electrodes are assembled onto a stretchable screen-printed current collector with an “island–bridge” configuration, which ensures conformal contact between the wearable BFC and the human body and endows the BFC with excellent performance stability under stretching condition. When applied to the arm of the volunteer, the BFC can generate a maximum power of 450 μW. When connected with a voltage booster, the on-body BFC is able to power a light emitting diode under both pulse discharge and continuous discharge modes during exercise. This demonstrates the promising potential of the flexible BP-based BFC as a self-sustained power source for next-generation wearable electronics.

development of wearable devices demands the development of efficient reliable and conformal power sources that can be easily integrated onto the human body. Despite the tremendous recent progress of wearable devices, most of these devices are still powered by rigid and bulky batteries, which pose environmental concerns. Enzymatic biofuel cells (BFCs), which rely on oxidoreductases to bioelectrocatalytically convert biofuels present in human body fluids, have been considered as promising candidates for powering next-generation wearable electronic devices.^[5,6] Specifically, epidermal skin-worn BFCs that use lactate as the substrate have been widely studied given the easy access to lactate in human sweat and their facile integration with wearable electronics.^[7–9] The power output of BFCs and their flexibility are two major challenges in this field considering the limited concentra-

1. Introduction

There is a continuously growing interest for wearable electronic devices, particularly, devices for fitness and health monitoring applications such as motion monitoring,^[1] physico-chemical signal sensing,^[2,3] and wound healing.^[4] The surging

tion of lactate in sweat and the external strain imposed from body movements. To overcome these issues, it is essential to develop electrode materials that can enhance enzyme electron transfer efficiency and provide flexibility and conformity when the device is mounted on the skin.


Carbon nanotubes (CNTs) have been widely used to construct bioelectrodes given their exceptional electronic properties, electrochemical inertness, and high surface area.^[10] To construct electrodes for practical biofuel cell applications, CNTs are often shaped into inks,^[11] pellets,^[8,12] papers,^[13,14] and fibers.^[15] Screen-printed CNT electrodes have been popular for wearable biofuel cells; however, this type of electrode requires mixing with an elastomeric binder, which inevitably blocks the active surface of CNTs and compromises power performance.^[11,16–18] CNT pellets, used in the first generation of implantable biofuel cells, are several millimeters thick and are therefore bulky, have slow mass transfer efficiency, and are fragile.^[19,20]

In this work, buckypaper (BP) was chosen as the electrode material. BP is a self-supported and conductive paper-like material comprising an entangled CNTs network.^[21] Previously, a buckypaper-based lactate/O₂ BFC was explored in synthetic tears.^[22] A buckypaper-based lactate bioanode coupled with a photocathode was very recently reported.^[23] However, the power density of both devices was rather low and

X. Chen, L. Yin, Dr. J. Lv, M. Le, N. G. Gutierrez, Y. Li, I. Jeerapan, Prof. S. Xu, Prof. J. Wang
Department of NanoEngineering
University of California San Diego
La Jolla, CA 92093, USA
E-mail: josephwang@ucsd.edu

X. Chen, Dr. A. J. Gross, Dr. F. Giroud, A. Berezovska, Dr. S. Cosnier
Département de Chimie Moléculaire
Université Grenoble Alpes-CNRS
UMR 5250, F-38000 Grenoble, France
E-mail: serge.cosnier@univ-grenoble-alpes.fr

Prof. R. K. O'Reilly
School of Chemistry
University of Birmingham
Birmingham B15 2TT, UK

 The ORCID identification number(s) for the author(s) of this article can be found under <https://doi.org/10.1002/adfm.201905785>.

DOI: 10.1002/adfm.201905785

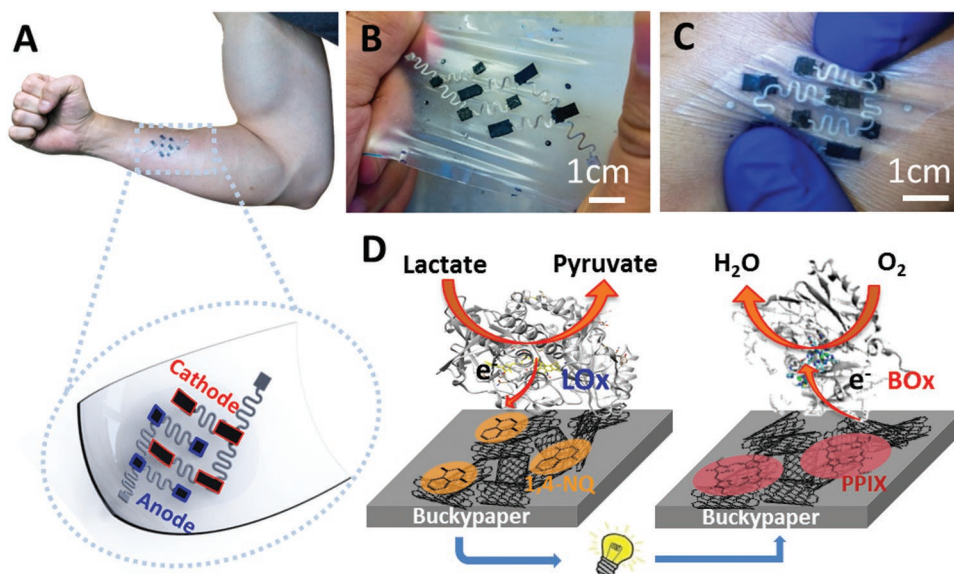


Figure 1. A) Photograph of the stretchable BFC device on a human arm; (zoom) schematic illustration of the skin-mountable wearable BFC device. B,C) Photographs of the BFC under stretching and bending, respectively. D) Schematics of the redox energy generation from sweat lactate oxidation at the anode and O_2 reduction at the cathode by BFC.

no stretchability was demonstrated. In both systems, multi-walled carbon nanotube (MWCNT) BP from a commercial source was utilized as the electrode material. In contrast, in the work reported herein, we fabricated lab-made MWCNT BP using a vacuum filtration method for use as the electrode material. A recent study shows that lab-made MWCNT BP is superior to commercial MWCNT BP as an immobilization matrix for bilirubin oxidase (BOx), which shows a higher catalytic current for the oxygen reduction reaction (ORR).^[24] A new class of lab-made flexible BPs has been developed in the Cosnier group based on the crosslinking of CNTs with polynorbornene linear polymers comprising pyrene groups. The polynorbornene-pyrene BP is an excellent matrix for redox mediator and enzyme immobilization.^[25,26] However, the lack of intrinsic stretchability has impeded the application of BPs in epidermal BFCs.

In this work, we present a high power, stretchable, flexible, and wearable BFC through a unique combination of highly conductive and catalytic BP electrodes with a structurally stretchable substrate to harvest energy from perspiration. To meet the requirement of wearable devices to endure rigorous movements and deformation during human exercise, a “two-degree” stretchability (i.e., structural stretchability and material intrinsic stretchability) was realized by combining a stretchable ink formula with an “island–bridge” architecture.^[11] The electrodes of the device were separated into “islands,” which are firmly bonded to the substrate, along with serpentine-shaped interconnecting “bridges,” which are soft and stretchable and can unwind under stress.^[11,27] When external strain is applied, the stress is distributed to the flexible “bridges” around the hard nonstretchable “islands,” therefore maintaining electrical resistance stability. Herein, a free-standing, buckling-enabled interconnect design, adopted from our previous work, was chosen to further enhance its flexibility and conductivity.^[27]

2. Results and Discussion

As illustrated in **Figure 1**, the stretchable and flexible wearable BFC is fabricated by integrating buckypaper-based electrodes and stretching current collectors. The stretchable substrate is fabricated via a high-throughput and low-cost screen-printing method. The carbon-based electrode “islands” are interconnected by high-conductivity silver composite “bridges” in a serpentine shape. A “skeleton” layer composed of polystyrene (PS) and styrene ethylene butylene styrene (SEBS) is added below the carbon islands to enhance their mechanical stability, and a water-soluble sacrificial layer is added below the serpentine interconnects to allow their separation from the substrate. A flexible polymer is printed on both sides of the silver interconnects to avoid the direct contact of silver and the electrolyte. The printed sacrificial layer is dissolved in water to enable buckling of the serpentine structures during deformation. To complete the assembly of the skin patch illustrated in **Figure 1A**, precut anodic and cathodic BP electrodes were thereafter attached to the carbon islands. A thin sheet of phosphate buffered solution-polyvinyl alcohol (PBS-PVA) hydrogel was added as electrolyte and a sweat reservoir was applied onto the electrodes. The fabrication process is illustrated in detail in **Figure S1** (Supporting Information).

The printed patch can be attached to the human epidermis in a wide range of locations where perspiration is usually observed (e.g., arm, neck, chest, and back) while maintaining high conformity (**Figure 1**). The system has been designed to endure mechanical strains caused by bodily movements. Endowed by the advantageous island–bridge structure, the BFC patch is highly flexible and stretchable (**Figure 1B**) and endures severe bending (**Figure 1C**). The serpentine structures can thus accommodate most of the stress. The patch can be activated once perspiration takes place a few minutes after exercise, where the

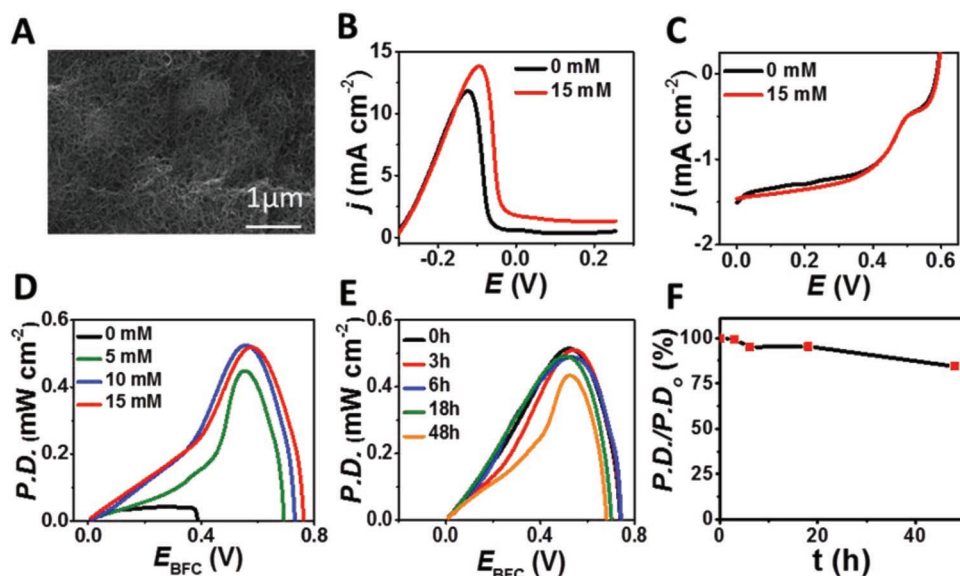


Figure 2. A) SEM image of buckypaper functionalized with pyrene-polynorbornene. B) LSV of the BP bioanode in the presence of (black) 0×10^{-3} M and (red) 15×10^{-3} M lactate in 0.5 M PBS (pH 7.4) at 5 mV s^{-1} . C) LSV of the BP biocathode in air-equilibrated buffer with (black) 0×10^{-3} M and (red) 15×10^{-3} M lactate at 5 mV s^{-1} . D) The power density versus voltage plots for the stretchable lactate BFC under different lactate concentrations ($0, 5, 10,$ and 15×10^{-3} M) in 0.5 M PBS (pH 7.4). E) Plots showing the stability of the stretchable BFC in the presence of 15×10^{-3} M lactate at different times up to 48 h. F) The calculated relative change of power density at 0.55 V over 48 h, based on the data in (E).

lactate in the sweat is absorbed into the hydrogel electrolyte and permeates to the electrodes. The reaction mechanism is illustrated in Figure 1D. The anode consists of a pyrene-polynorbornene functionalized BP with immobilized lactate oxidase (LOx) to catalyze the oxidation of lactate into pyruvate with 1,4-naphthoquinone (1,4-NQ) as the electron transfer mediator. The cathode consists of BPs with immobilized BOx from *Myrothecium sp.* to catalyze the ORR. For the cathode, BP is modified with protoporphyrin IX (PPIX) molecules that can orientate the enzyme preferentially with the T1 center of BOx to facilitate direct electron transfer with the CNTs.^[14,28] The current and voltage generated from the anodic and cathodic reactions can thereafter be exploited to power various electronics in a biofuel cell configuration.

The morphology of BP functionalized with the pyrene-polynorbornene homopolymer was characterized using scanning electron microscope (SEM) and revealed a homogenous mesoporous structure of entangled CNT bundles (Figure 2A). The electrochemical performance of the biocathode and bioanode was evaluated individually using a three-electrode setup with a platinum (Pt) counter electrode and a Ag/AgCl (3 M KCl) reference electrode. Figure 2B shows overlaid linear sweep voltammograms (LSVs) recorded for the bioanode in the presence of 0 and 15×10^{-3} M lactate in 0.5 M PBS (pH 7.4), respectively. Upon addition of lactate, the mediated bioelectrocatalytic current of lactate oxidation starts to flow and results in a current density of 1.3 mA cm^{-2} at 0.2 V. Figure 2C shows LSVs for the biocathode. The oxygen reduction current starts to increase dramatically at a potential close to 0.5 V, reaching a maximum current density of -1.5 mA cm^{-2} at 0 V. The presence of lactate did not affect the performance of the BOx bioelectrode as the onset potential for ORR and the limiting current were unchanged.

The high onset potential and steep oxygen reduction reaction slope indicate a more efficient direct electron transfer between the T1 center of BOx and the CNTs. The excellent performance is in accordance with other reported protoporphyrin-modified biocathodes.^[14,28]

The power performance of the BFC was investigated using a unit cell device comprising a single biocathode and a single bioanode, as depicted in Figure 1D. As low oxygen concentration can limit the power of the BFC, the area of the biocathode was designed to be two times larger than the bioanode to ensure that the BFC performance was not limited by the cathode. LSVs were recorded from the open circuit voltage (OCV) to 0.01 V in different lactate concentrations. The power–voltage curves are shown in Figure 2D. Both the OCV and peak power density increased with increasing lactate concentrations, reaching saturation at 10×10^{-3} M lactate. A maximum power density of 0.5 mW cm^{-2} was recorded at 0.55 V in 10×10^{-3} M lactate. However, for subsequent characterization experiments, 15×10^{-3} M lactate was chosen to match the average lactate concentration in sweat.^[29] Although the power density in this work is lower than the maximum value of $\approx 1.2 \text{ mW cm}^{-2}$ reported previously,^[8] an oxygen reducing enzymatic biocathode was used instead of a battery-type silver oxide cathode. The power performance was compared with other reported work in the literature and is summarized in Table S1 (Supporting Information). The power performance stability of the BFC was investigated periodically by performing linear sweep voltammetry (LSV) in 15×10^{-3} M lactate over an extended period of 48 h (Figure 2E). As shown in Figure 2F, the power density at 0.55 V decreases only by 16% after 48 h. Control power–voltage curves of BFCs fabricated by immobilizing enzymes on screen-printed current collectors and CNT ink^[9] electrodes are included in Figures S2

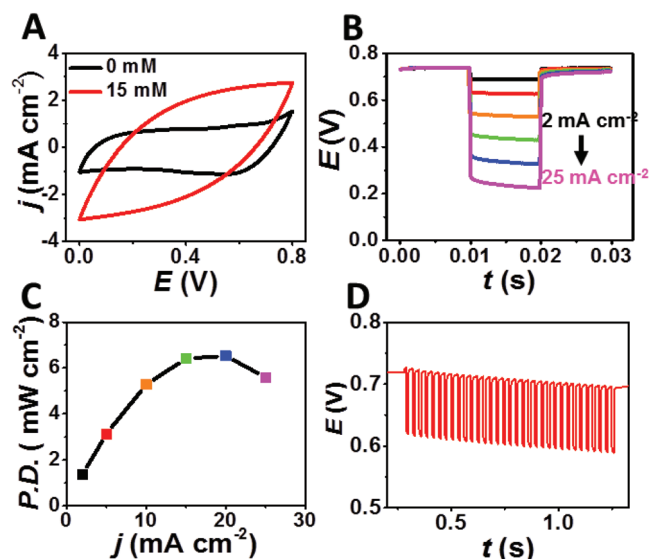


Figure 3. A) CV of BFC in the presence of (black) 0×10^{-3} M and (red) 15×10^{-3} M lactate in 0.5 M PBS (pH 7.4) at 50 mV s^{-1} . B) Overlay of potential profiles obtained from BFC discharge at 2, 5, 10, 15, 20, and 25 mA cm^{-2} over 10 ms. C) Plot of the calculated pulse power density as a function of the discharge current density. D) Potential profile of the BFC during a discharge at 5 mA cm^{-2} at 33 Hz frequency.

and S3 (Supporting Information), respectively. For these two alternative systems, the power performance in 15×10^{-3} M lactate is negligible compared to the BP-based BFC, highlighting that the excellent performance of BFC originates from the BPs used in the present work.

The ability of the BFC to function also as a self-powered supercapacitor was investigated. **Figure 3A** shows cyclic voltammograms (CVs) recorded for the BFC in the presence of 0×10^{-3} M and 15×10^{-3} M lactate in PBS. A quasi-symmetric rectangular shape of the CV curves indicates highly capacitive behavior, which is expected for high surface area nanostructured carbon electrodes.^[12,30] Upon addition of 15×10^{-3} M lactate, the capacitive current increased, which can be explained by the additional electronic loading on the CNT matrix via the enzymatic oxidation of lactate. The capacitance of the device was further investigated by performing galvanostatic charge–discharge (GCD) at different current densities. GCD curves and the calculated areal capacitance at different current densities are shown in **Figure S4** (Supporting Information). A high capacitance of 40 mF cm^{-2} was observed at 0.1 mA cm^{-2} , which is comparable to other reported self-charging biosupercapacitors.^[31,32] We note that no extra modification of the bioelectrodes was needed, such as manganese oxide to obtain this capacitive performance. Current pulse chronopotentiometry was performed to evaluate the BFC power performance in pulse operation mode. **Figure 3B** shows the overlay of potential profiles of the BFC discharged at 2 to 25 mA cm^{-2} over 10 ms. The potential profile at all discharge current densities showed the same feature, with an initial IR drop followed by a capacitive discharge and then the self-recharge back to its original voltage after the pulse. The calculated pulse power delivered by the BFC is shown in **Figure 3C**, reaching a maximum power of 6.5 mW cm^{-2} at 20 mA cm^{-2} . This value is around 13 times higher than the power delivered in normal BFC mode. The BFC also shows high

stability at high frequency discharge. As shown in **Figure 3D**, the BFC is discharged at 5 mA cm^{-2} at 33 Hz frequency (10 ms discharge and 20 ms rest) and the OCV only decreases slightly.

To highlight the resiliency of the BP-based “island–bridge” BFC, we examined its performance under severe mechanical distortions (**Figure 4**). The elastic and highly conductive silver composite ink is chosen as the “bridges” to minimize the power loss due to high connection resistance, and the serpentine structure is implemented to avoid increased strain-induced resistance during deformation by enabling buckling.^[9,11,27,33] The mechanical stability of the buckypaper BFC was evaluated using a stepping-motor controlled biaxial stretching stage. The printed BFC is stretched repeatedly to 120% of its original size in both directions (**Figure 4B**). The resistance of the circuit between the silver contact on the end of the patch and the central printed carbon electrode is measured during a 100-cycle stretching test, as shown in **Figure 4C**. The resistance of the circuit varies less than 1Ω in each stretching cycle (**Figure 4C**, inset), with no trend of increasing resistance after all of the stretching cycles. The mechanical stability was further validated by monitoring the discharge current of the BFC under a constant load. One pair of electrodes was covered in PBS-PVA gel electrolyte with 15×10^{-3} M lactate and connected to a $33 \text{ k}\Omega$ resistor, as shown in **Figure 4A**. The discharge current exhibits no significant change during 20 cycles of stretching, which further validates the mechanical stability of the patch as a practical wearable energy-harvesting device. The durability of the generated power performance was examined in connection to numerous stretching cycles. A LSV scan was performed every 20 cycles of 20% biaxial stretching. The power density remained highly stable after 100 cycles of stretching (**Figure 4E,F**).

The real-time power output of the wearable buckypaper BFC was tested by monitoring the current of the circuit (with 510Ω load) when the volunteer was doing stationary cycling exercise. The power change of the BFC during the whole process is shown in **Figure 5A**. The power is very low before the volunteer started to sweat due to the absence of the fuel. After 10 min of exercise, perspiration is visually observed on the subject, which is corroborated by a rapid increase in the power density of the BFC indicating lactate molecules from the sweat were transferred to the interface of the LOx bioanode. The highest power density obtained is around $450 \mu\text{W}$ after 30 min of perspiration, which is an output that is sufficient to power various wearable devices considering their low power requirements.^[34] When the volunteer stopped cycling, a constant drop of power is observed, probably caused by the insufficient supply of lactate and oxygen dissolved in the sweat.^[16] The capability of the flexible buckypaper BFC to serve as the power source for wearable electronic devices was demonstrated by powering an LED during stationary cycling exercise. The voltage of the BFC was boosted using a flexible DC–DC converter, as shown in **Figure 5C**, and **Figure S6** and **Videos S1** and **S2** of the Supporting Information. **Figure 5B** illustrates the circuit connection of the patch, the voltage booster, the LED, and a switch that was used to control the “on” and “off” function of the LED. When connected with the sweat-based BFC, the LED lit up (**Figure 5E**) and its voltage can reach over 1.4 V both in pulse mode and continuous discharging modes

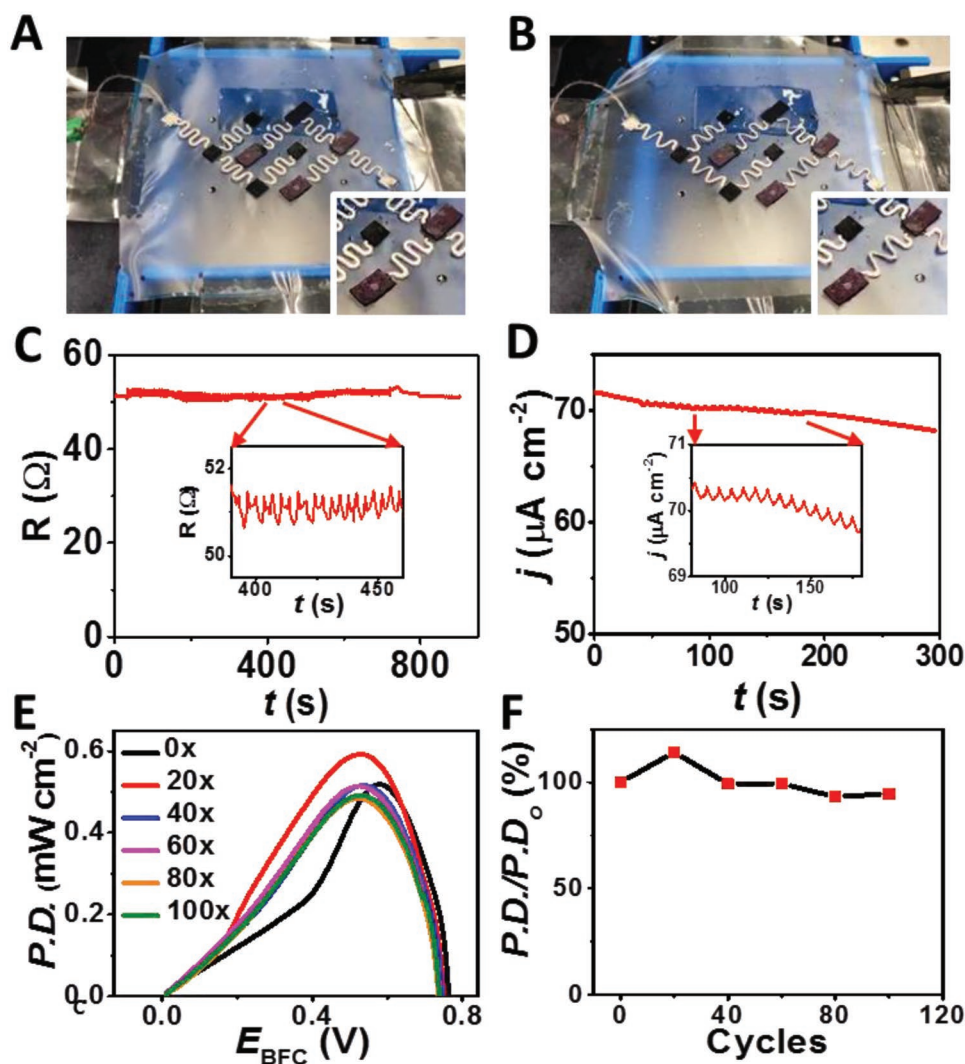


Figure 4. Mechanical resilience studies: Image of the wearable BFC A) before and B) after 20% stretching. C) Resistance profile obtained during 20% stretching; (inset) zoom of resistance fluctuations. D) Current density output profile of the BFC under a 33 k Ω load in PVA gel immersed in 15×10^{-3} M lactate; (inset) zoom of current density fluctuations. E) Plots of BFC power density versus voltage under 20% stretching for 0, 20, 40, 60, 80, and 100 cycles in 15×10^{-3} M lactate. F) The calculated relative change of power density at 0.55 V over 100 stretching cycles.

(Figure S5, Supporting Information), illustrating the feasibility of the voltage boosted buckypaper BFCs to supply energy for wearable electronics.

3. Conclusion

In summary, a stretchable and wearable enzymatic BFC that harvests energy from sweat has been created through the combination of a screen-printed current collector substrate and flexible enzyme-modified polynorbornene-based BPs. During in vitro experiments, the assembled BFC had a high OCV of 0.74 V and a maximum power density of $520 \mu\text{W cm}^{-2}$. The stretchability of the device was realized through the coupling of an “island-bridge” architecture and strain-enduring inks. The device was able to retain its performance stability under multiple stretching cycles. After coupling with a voltage booster, the BP-based BFC

was able to power a commercial LED both in pulse mode and in continuous mode. We have demonstrated the promising potential of using BP as a high-performance carbon electrode material for epidermal BFC with a stretchable supporting substrate. Such stretchable skin-worn devices are expected to contribute to the development of epidermal energy harvesting systems and wearable electronics, in general. The reported BFC device still relies on exercise for sweat generation, which limits its usages for athletic purposes. The lactate (fuel) sweat concentration, and hence the generated power, may depend on the specific individual and their activity. Challenges, such as the availability of biofuels or oxygen, can be addressed via different strategies such as the use of sweat-inducing chemicals or replacing the cathode with an air-breathing electrode. Future studies will aim at improving the biocompatibility, the catalytic anode performance of each individual bioelectrode, and further electronics integration along with extensive on-body operations.

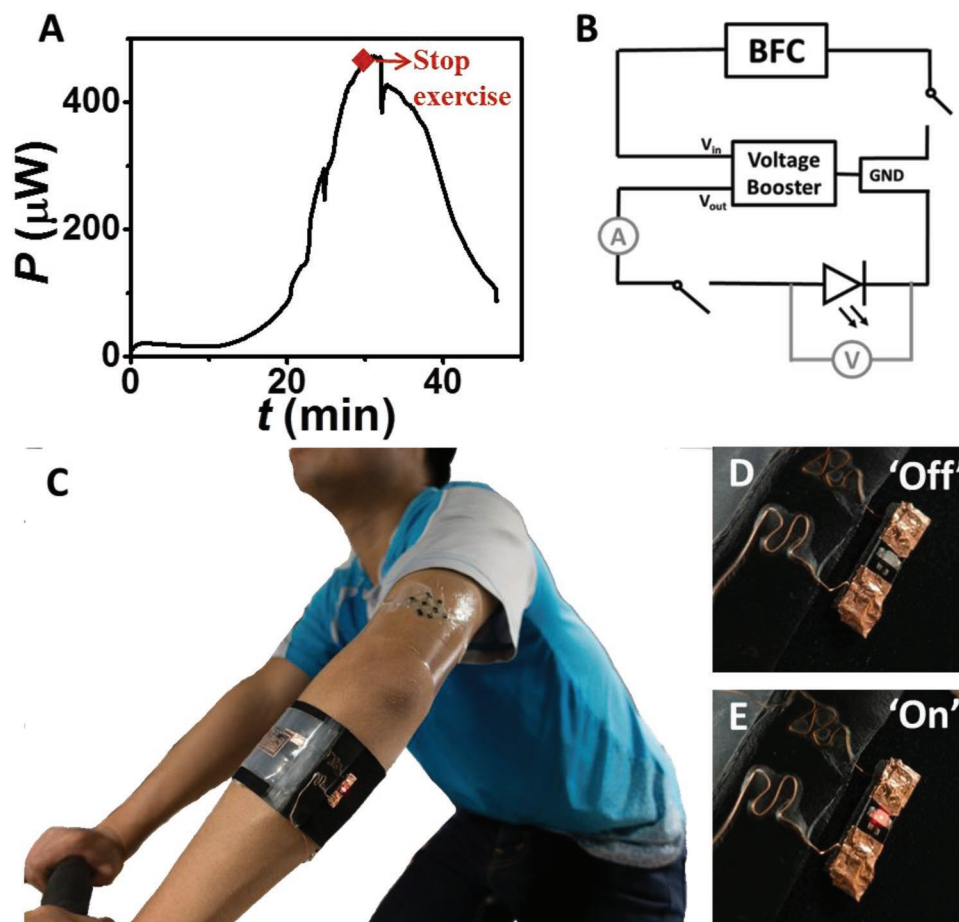


Figure 5. A) Power output profile under 510 Ω load during an on-body experiment. B) The circuit schematics for using the flexible and stretchable epidermal BFC patch to power an LED via a flexible DC–DC convertor. C) Image of on-body experiment setup with a BFC mounted on the arm of the volunteer. D,E) Images of the LED switched on and off, respectively.

4. Experimental Section

Chemicals and Reagents: 1,4-NQ, PPIX ($\geq 95\%$), bovine serum albumin (BSA), glutaraldehyde, chitosan, toluene, L(+)-lactic acid, potassium phosphate dibasic, potassium phosphate monobasic, PVA (M_w 146 000–186 000 and M_w 89 000–98 000), potassium hydroxide, ethanol, acetone, acetic acid, *N,N*-dimethylformamide (DMF, 99.9%), and Ag flakes (10 μm) were purchased from Sigma-Aldrich. Tetrahydrofuran was purchased from EMD Millipore. Hydroxyl-functionalized multi-walled carbon nanotubes (MWCNT-OHs, $\text{Ø} = 10\text{--}20$ nm, 10–30 μm length, $>95\%$ purity) were purchased from Cheap Tubes Inc. Commercial grade MWCNTs ($\text{Ø} = 9.5$ nm, 1.5 μm length, $\geq 90\%$ purity) for buckypaper fabrication were purchased from Nanocyl. L-Lactate oxidase (LOx) from “microorganism” was purchased from Toyobo. BOx from *Myrothecium sp.* was a gift from Amano Enzyme. Polyurethane (PU, Tecoflex SG-80A) was purchased from Lubrizol LifeSciences. PS was obtained from polystyrene foam packaging material. SEBS copolymer was purchased from Kraton. Ecoflex 00-30 (Smooth-On, Inc. PA.) was prepared by mixing equal volumes of prepolymers A and B, provided by the supplier. Perme-Roll Lite (L34R10) was purchased from Nitto Denko. Carbon paste (C2030519P4) was purchased from Gwent Group. 0.5 M pH 7.4 potassium PBS was prepared from potassium phosphate dibasic and potassium phosphate monobasic. Ultrapure deionized (DI) water (18.2 M Ω) was used for all of the aqueous solutions.

“Island–Bridge” Electrode Fabrication: A thin layer of Ecoflex was printed on the adhesive side of a Perme-Roll Lite film and cured at 65 $^{\circ}\text{C}$ for 10 min to form the low elastic modulus substrate. Each layer

depicted in Figure S1 (Supporting Information) was screen printed on the nonadhesive side of the elastic substrate using an MPM-SPM semi-automatic screen printer (Speedline Technologies, Franklin, MA, USA). A 100 μm thick stainless steel printing stencil was designed in AutoCAD (Autodesk, USA) and laser-cut (Metal Etch Services, San Marcos, CA, USA). Formulations of inks used for each layer are provided in the Supporting Information. The printing steps are as follow: first, to enhance the adhesion, a PU interlayer was printed on top of the substrate and cured at 60 $^{\circ}\text{C}$ for 15 min. Thereafter, a rigid “island-like” structure layer was printed using the PS-SEBS ink onto the modified stretchable film and cured at 65 $^{\circ}\text{C}$ for 15 min. Then, the sacrificial layer was printed using PVA and cured at 80 $^{\circ}\text{C}$ for 10 min. A stretchable insulating serpentine “bridge-like” structure layer was then printed using the SEBS ink and cured at 65 $^{\circ}\text{C}$ for 15 min. A stretchable conductive serpentine “bridge-like” structure layer was subsequently printed using the Ag-SEBS ink and cured at 65 $^{\circ}\text{C}$ for 15 min. Then another insulating layer was printed on top of the silver pattern using the SEBS ink and cured at 65 $^{\circ}\text{C}$ for 15 min. Then a rigid conductive “island-like” layer was printed on top of the PS-SEBS using commercial carbon paste and left to dry at room temperature and then cured at 60 $^{\circ}\text{C}$ for 15 min. Then, a backbone serpentine layer was printed using the PS-SEBS ink and cured at 65 $^{\circ}\text{C}$ for 15 min. Finally, the sacrificial layer was removed by dissolving in DI water. Conductive stainless steel thin conductive threads (Adafruit, NY, USA) were attached to the contact points of the device using Ag-SEBS inks. The contact points were then insulated using PS-SEBS ink.

Fabrication of the Polynorbornene-Pyrene Buckypaper: The polynorbornene homopolymer with pyrene groups ((P)₅₀), M_n ,

SEC = 10.2 kg mol⁻¹, $D_{SEC} = 1.22$) was synthesized as previously reported via ring opening metathesis polymerization.^[35] 66 mg of MWCNTs was dispersed in 66 mL of DMF, followed by sonication for 30 min. 6.6 mg of the polymer was added to the suspension. The suspension was then sonicated for a further 30 min. The as-prepared suspension was filtrated using a diaphragm pump (MZ 2C NT model, Vacuubrand) on a Millipore PTFE filter (JHWP, 0.45 μ m pore size). The resulting BP was rinsed with water, left under vacuum for 1 h, and then left to dry in air overnight.

Assembly of the Buckypaper Biofuel Cell: For anode preparation, the BP was first cut into a square electrodes (3 × 3 mm). 5 μ L of 5 mg mL⁻¹ MWCNT-OHs dispersed in 0.2 M 1,4-NQ in 9:1 vol/vol ethanol/acetone solution was dropcasted onto the cut BP electrode surface. For the cathode, the BP was cut into rectangular electrodes (3 × 6 mm). 10 μ L of 40 × 10⁻³ M PPIX in 9:1 vol/vol ethanol/acetone solution was dropcasted onto the cut BP electrode surface. The modified BP was then left to dry in air. Carbon paste was subsequently used to glue individual BPs onto screen-printed carbon “islands” and left to dry in an oven at 50 °C for 30 min. Thereafter, the cathodic BP was functionalized by dropcasting 10 μ L of 40 mg mL⁻¹ BOx in PBS. The anodic BP was first rinsed with PBS to remove loosely bound 1,4-NQ, and then followed by dropcasting 5 μ L of a mixture of 40 mg mL⁻¹ LOx and 10 mg mL⁻¹ BSA. 3 μ L of 1% glutaraldehyde solution was then dropcasted onto the surface followed by dropcasting 3 μ L of 1 wt% chitosan in 0.1 M acetic acid. The BFC device was then left to dry overnight at 4 °C.

Characterization of the Materials: The morphology of the BP was characterized using scanning electron microscope (Phillips XL30 ESEM) with an accelerating voltage of 20 kV.

Electrochemical Measurements: The electrochemical performances of the half cells and BFC were conducted using a μ Autolab Type II commanded by Nova software (Version 2.1). In vitro table-top electrochemical characterization was performed in 0.5 M pH 7.4 PBS. The enzyme-catalyzed lactate oxidation and oxygen reduction reactions at the bioanode and biocathodes were characterized by LSV in a three-electrode system with a scan rate of 5 mV s⁻¹. The three-electrode system consisted of a BP electrode as the working electrode, a Pt wire as the counter electrode, and an Ag/AgCl (3 M KCl) as the reference electrode. The assembled BFC device was characterized in a two-electrode system with the bioanode as the counter and reference electrode and the biocathode as the working electrode. Linear sweep polarization curves of the BFC in different lactate concentrations were obtained by scanning from OCV to 0.01 V at 5 mV s⁻¹. The calculation of the power density of a single BFC was based on the geometrical area of the cathode (0.18 cm²). CV and GCD techniques were used to characterize the capacitive behavior of the BFC. CVs were performed from 0 to 0.8 V with a scan rate of 50 mV s⁻¹, while the GCD tests were carried out at current densities of 0.1, 0.2, 0.5, and 1 mA cm⁻². The capability of the BFC to serve as the pulse generator was characterized by chronopotentiometry. The minimum voltage at the end of each 10 ms pulse discharge was used to calculate the power density.

Mechanical Resilience Studies: The mechanical resiliency studies were conducted on a motorized linear stage connected to a controller (A-LST0250A-E01 Stepper Motor and Controller, Zaber Technologies, Vancouver, Canada). Four linear motors with the same speed were used to conduct 20% biaxial stretching. The stability of the BFC during the mechanical deformations was studied by measuring the resistance of the screen-printed current collector and the current output of the BFC with a 33 k Ω loading during 20% biaxial stretching.

Fabrication of the DC Voltage Booster Circuit: A layer of poly(methyl methacrylate) (PMMA) (495K, A6) was coated onto a glass slide at a speed of 1500 rpm for 20 s, and then cured by baking for 150 °C on a hotplate for 1 min. Afterward, an Ecoflex (Smooth-On, 1:1) layer of 100 μ m thickness was coated on top of the PMMA and cured at room temperature for 2 h. On a separate glass slide, a layer of polydimethylsiloxane (PDMS, Sylgard 184 silicone elastomer, 20:1) was coated at 3000 rpm for 30 s, followed by curing in an oven at 150 °C for 30 min. A Cu sheet (20 μ m thick, Oak-Mitsui Inc.) was coated with PI (from poly(pyromellitic dianhydride-co-4,40-oxydianiline) amic acid solution, PI2545 precursor; HD Microsystems) at 4000 rpm for 60 s, soft baked on a hotplate

at 110 °C for 3 min, 150 °C for 1 min, and finally cured in a nitrogen oven at 300 °C for 1 h. This Cu sheet was transferred on top of the PDMS/glass substrate. The interconnect layout, designed in AutoCAD, was patterned onto the Cu sheet via laser ablation. A laser (wavelength 1064 nm, pulse energy 0.42 mJ, pulse width 1 μ s, frequency 35 KHz, and mark speed 500 mm s⁻¹) ablated the Cu sheet into the designed pattern, and residual Cu material was removed. The Cu pattern was picked off the substrate with water soluble tape (3M Inc.) and transferred onto the prepared PMMA/Ecoflex/glass substrate. The water soluble tape was removed by room-temperature tap water. The Cu interconnections were cleaned by flux (WOR331928, Worthington Inc.) for removal of surface oxides. Sn42Bi57.6Ag0.4 alloy paste (Chip Quick Inc., SMDLTLFP-ND, low melting point 138 °C) was used to solder the chip components (including the BQ25504 Ultra Low-Power Boost Converter for Energy Harvesting, Texas Instruments) onto the Cu interconnects, followed by baking on a hotplate at \approx 150 °C for 4 min, and then cooling to room temperature. Finally, the entire surface of the circuit was encapsulated by Ecoflex with 1 mm thickness and cured at room temperature for 4 h. The combined Ecoflex/Cu interconnect/circuit device was then removed from the glass/PMMA substrate using a razor blade.

On-Body Power Generation: The flexible buckypaper BFC was mounted on the arm of one volunteer with the assistance of an adhesive film (Perme-Roll). The stainless conductive steel yarn was used to connect the BFC and a 510 Ω resistor to reach the maximal power density, with stretchable Ag ink as the joint bonding resin. The current of the circuit was record every 5 s by a potentiostat during which the volunteer was doing stationary cycling. The capability of the BFC to power one LED was demonstrated by using the flexible DC–DC converter to boost the voltage and a switch to control the “on” and “off” status. The voltage of the LED was tested in both pulse and continuous working mode. All on-body experiments were approved by the Human Research Protections Program at University of California, San Diego, and followed the guidelines of institutional review boards.

Supporting Information

Supporting Information is available from the Wiley Online Library or from the author.

Acknowledgements

X.C., L.Y., and J.L. contributed equally to this work. X.C. is grateful for a Université Grenoble Alpes Ph.D. scholarship and IDEX travel grant. J.W. acknowledges support from the Defense Threat Reduction Agency Joint Science and Technology Office for Chemical and Biological Defense (HDTRA 1-16-1-0013) and the Army SBIR Program. I.J. acknowledges support from Thai Development and Promotion of Science and Technology Talents Project (DPST). A.B. is grateful to the Auvergne-Rhône-Alpes for Ph.D. funding. The authors acknowledge support from the platform “Surfaces Functionalization and Transduction” of the scientific structure “Nanobio” for providing facilities.

Conflict of Interest

The authors declare no conflict of interest.

Keywords

bioelectrocatalysis, energy harvesting, flexible electronics, paper electrode, screen printing

Received: July 17, 2019
Revised: August 22, 2019
Published online:

- [1] J. Lv, C. Kong, C. Yang, L. Yin, I. Jeerapan, F. Pu, X. Zhang, S. Yang, Z. Yang, *Beilstein J. Nanotechnol.* **2019**, *10*, 475.
- [2] A. J. Bandothkar, I. Jeerapan, J. Wang, *ACS Sens.* **2016**, *1*, 464.
- [3] J. Kim, I. Jeerapan, J. R. Sempionatto, A. Barfidokht, R. K. Mishra, A. S. Campbell, L. J. Hubble, J. Wang, *Acc. Chem. Res.* **2018**, *51*, 2820.
- [4] J. Banerjee, P. Das Ghatak, S. Roy, S. Khanna, E. K. Sequin, K. Bellman, B. C. Dickinson, P. Suri, V. V. Subramaniam, C. J. Chang, C. K. Sen, *PLoS One* **2014**, *9*, e89239.
- [5] A. J. Bandothkar, J. Wang, *Electroanalysis* **2016**, *28*, 1188.
- [6] M. Rasmussen, S. Abdellaoui, S. D. Minter, *Biosens. Bioelectron.* **2016**, *76*, 91.
- [7] A. Koushanpour, M. Gamella, E. Katz, *Electroanalysis* **2017**, *29*, 1602.
- [8] A. J. Bandothkar, J.-M. You, N.-H. Kim, Y. Gu, R. Kumar, A. M. V. Mohan, J. Kurniawan, S. Imani, T. Nakagawa, B. Parish, M. Parthasarathy, P. P. Mercier, S. Xu, J. Wang, *Energy Environ. Sci.* **2017**, *10*, 1581.
- [9] J. Lv, I. Jeerapan, F. Tehrani, L. Yin, C. A. Silva-Lopez, J.-H. Jang, D. Joshua, R. Shah, Y. Liang, L. Xie, F. Soto, C. Chen, E. Karshalev, C. Kong, Z. Yang, J. Wang, *Energy Environ. Sci.* **2018**, *11*, 3431.
- [10] J. J. Gooding, *Electrochim. Acta* **2005**, *50*, 3049.
- [11] A. J. Bandothkar, I. Jeerapan, J.-M. You, R. Nuñez-Flores, J. Wang, *Nano Lett.* **2016**, *16*, 721.
- [12] C. Agnès, M. Holzinger, A. Le Goff, B. Reuillard, K. Elouarzaki, S. Tingry, S. Cosnier, *Energy Environ. Sci.* **2014**, *7*, 1884.
- [13] L. Hussein, G. Urban, M. Krüger, *Phys. Chem. Chem. Phys.* **2011**, *13*, 5831.
- [14] A. J. Gross, X. Chen, F. Giroud, C. Abreu, A. Le Goff, M. Holzinger, S. Cosnier, *ACS Catal.* **2017**, *7*, 4408.
- [15] C. H. Kwon, S.-H. Lee, Y.-B. Choi, J. A. Lee, S. H. Kim, H.-H. Kim, G. M. Spinks, G. G. Wallace, M. D. Lima, M. E. Kozlov, R. H. Baughman, S. J. Kim, *Nat. Commun.* **2014**, *5*, 3928.
- [16] W. Jia, G. Valdés-Ramírez, A. J. Bandothkar, J. R. Windmiller, J. Wang, *Angew. Chem., Int. Ed.* **2013**, *52*, 7233.
- [17] W. Jia, X. Wang, S. Imani, A. J. Bandothkar, J. Ramírez, P. P. Mercier, J. Wang, *J. Mater. Chem. A* **2014**, *2*, 18184.
- [18] I. Jeerapan, J. R. Sempionatto, A. Pavinatto, J.-M. You, J. Wang, *J. Mater. Chem. A* **2016**, *4*, 18342.
- [19] A. Zebda, C. Gondran, A. Le Goff, M. Holzinger, P. Cinquin, S. Cosnier, *Nat. Commun.* **2011**, *2*, 370.
- [20] A. Zebda, S. Cosnier, J.-P. Alcaraz, M. Holzinger, A. Le Goff, C. Gondran, F. Boucher, F. Giroud, K. Gorgy, H. Lamraoui, P. Cinquin, *Sci. Rep.* **2013**, *3*, 1516.
- [21] A. J. Gross, M. Holzinger, S. Cosnier, *Energy Environ. Sci.* **2018**, *11*, 1670.
- [22] R. C. Reid, S. D. Minter, B. K. Gale, *Biosens. Bioelectron.* **2015**, *68*, 142.
- [23] Y. Yu, J. Zhai, Y. Xia, S. Dong, *Nanoscale* **2017**, *9*, 11846.
- [24] X. Chen, A. J. Gross, F. Giroud, M. Holzinger, S. Cosnier, *Electroanalysis* **2018**, *30*, 1511.
- [25] A. J. Gross, M. P. Robin, Y. Nedellec, R. K. O'Reilly, D. Shan, S. Cosnier, *Carbon* **2016**, *107*, 542.
- [26] L. Fritea, A. J. Gross, K. Gorgy, R. K. O'Reilly, A. Le Goff, S. Cosnier, *J. Mater. Chem. A* **2019**, *7*, 1447.
- [27] L. Yin, J. K. Seo, J. Kurniawan, R. Kumar, J. Lv, L. Xie, X. Liu, S. Xu, Y. S. Meng, J. Wang, *Small* **2018**, *14*, 1800938.
- [28] N. Lalaoui, A. Le Goff, M. Holzinger, S. Cosnier, *Chem. - Eur. J.* **2015**, *21*, 16868.
- [29] C. J. Harvey, R. F. LeBouf, A. B. Stefaniak, *Toxicol. In Vitro* **2010**, *24*, 1790.
- [30] D. Pankratov, P. Falkman, Z. Blum, S. Shleev, *Energy Environ. Sci.* **2014**, *7*, 989.
- [31] D. Pankratov, Z. Blum, D. B. Suyatin, V. O. Popov, S. Shleev, *ChemElectroChem* **2014**, *1*, 343.
- [32] D. Pankratov, F. Conzuelo, P. Pinyou, S. Alsaoub, W. Schuhmann, S. Shleev, *Angew. Chem., Int. Ed.* **2016**, *55*, 15434.
- [33] L. Yin, R. Kumar, A. Karajic, L. Xie, J. You, D. Joshua, C. S. Lopez, J. Miller, J. Wang, *Adv. Mater. Technol.* **2018**, *3*, 1800013.
- [34] S. Gong, W. Cheng, *Adv. Energy Mater.* **2017**, *7*, 1700648.
- [35] S. Cosnier, R. Haddad, D. Moatsou, R. K. O'Reilly, *Carbon* **2015**, *93*, 713.